

# Instrument for simultaneous measurement of Seebeck coefficient and thermal conductivity in the temperature range 300–800 K with Python interfacing

Cite as: Rev. Sci. Instrum. 93, 043902 (2022); doi: 10.1063/5.0061819

Submitted: 30 June 2021 • Accepted: 18 March 2022 •

Published Online: 6 April 2022



View Online



Export Citation



CrossMark

Shamim Sk,<sup>1,a</sup> Abhishek Pandey,<sup>1</sup> and Sudhir K. Pandey<sup>2,b</sup>

## AFFILIATIONS

<sup>1</sup> School of Basic Sciences, Indian Institute of Technology Mandi, Kamand 175075, India

<sup>2</sup> School of Engineering, Indian Institute of Technology Mandi, Kamand 175075, India

<sup>a</sup>Author to whom correspondence should be addressed: shamimsk20@gmail.com

<sup>b</sup>Electronic mail: sudhir@iitmandi.ac.in

## ABSTRACT

Fabrication and characterization of an instrument for the high-temperature simultaneous measurement of the Seebeck coefficient ( $S$ ) and thermal conductivity ( $\kappa$ ) have been carried out with Python automation. The steady-state-based Fourier's law of thermal conduction is employed for  $\kappa$  measurement. The parallel thermal conductance technique is implemented for heat loss measurement. Introducing a thin heater and insulating heater base minimizes the heat loss and makes it easier to arrive at high temperatures. Measurement of  $S$  is carried out using the differential method. The same thermocouples are used to measure the temperature as well as voltage for  $S$  measurement. Care of temperature dependent  $S$  of the thermocouple has also been taken. Simple design, small size, and lightweight make this instrument more robust. All the components for making a sample holder are easily available in the market and can be replaced as per the user's demand. This instrument can measure samples with various dimensions and shapes in the temperature range 300–800 K. The instrument is validated using different classes of samples, such as nickel, gadolinium, Fe<sub>2</sub>VAI, and LaCoO<sub>3</sub>. A wide range of  $S$  values from  $\sim -20$  to  $\sim 600 \mu\text{V/K}$  and  $\kappa$  values from  $\sim 1.1$  to  $\sim 23.5 \text{ W/m K}$  are studied. The measured values of  $S$  and  $\kappa$  are in good agreement with the reported data.

Published under an exclusive license by AIP Publishing. <https://doi.org/10.1063/5.0061819>

## I. INTRODUCTION

Fast consumption of natural energy sources (e.g., coal, oil, and gas) has always pushed researchers to find alternative sources of energy. In this context, a thermoelectric generator (TEG) is a prominent candidate, which can convert the industrial waste heat into useful electricity.<sup>1,2</sup> TEG is characterized by means of a dimensionless parameter, called *figure-of-merit* ( $ZT$ ),<sup>3</sup>

$$ZT = \frac{S^2 \sigma T}{\kappa}, \quad (1)$$

where  $S$ ,  $\sigma$ , and  $\kappa$  are the Seebeck coefficient, electrical conductivity, and thermal conductivity, respectively. Here,  $T$  is the absolute

temperature of the sample. Efficient thermoelectric (TE) materials should possess high values of  $S$  and  $\sigma$  along with a low value of  $\kappa$  to attain a high  $ZT$ . For the calculation of  $ZT$ , these three parameters are required to be measured. Out of these three,  $\kappa$  is most challenging to measure especially in a high-temperature region due to the undefined amount of heat loss by conduction, convection, and radiation. From Eq. (1), it is seen that unlike the linear dependence of  $S$  over other quantities,  $ZT$  is proportional to the square of  $S$ . Therefore, any small error in the measurement of  $S$  can significantly affect the value of  $ZT$ . Hence, precise measurement of  $S$  is crucial to acquire  $ZT$  with a good accuracy limit.

$S$  is simply defined as the generation of electrical voltage in the presence of a temperature gradient.  $S$  can be measured in two ways:

integral and differential. In the integral method, the temperature at one end of the sample is varied, whereas the other end of the sample is kept at a constant temperature. To maintain this constant temperature, an extra cooling system is required, which makes the instrument more complex and costly. Furthermore, this method is also not suitable for nondegenerate semiconductors and insulators.<sup>4,5</sup> On the other hand, in the differential method,  $S$  of a sample is calculated by  $S = -\frac{\Delta V}{\Delta T} + S_{\text{wire}}$ , where  $\Delta V$  is the induced voltage difference across the temperature difference  $\Delta T$  within a sample and  $S_{\text{wire}}$  is the Seebeck coefficient of the connecting wire. Most of the Seebeck measuring instruments prefer to use this method because of its simplicity and no additional requirement of a cooling system.<sup>6–9</sup> In this method, the connecting wire and thermocouple should be attached at the same point of a sample to measure the temperature and induced voltage, which makes this method more challenging.<sup>5</sup> To overcome this issue, de Boor and Muller<sup>10</sup> came up with a different approach under the differential method, where the same thermocouple is used for the measurement of the temperature as well as induced voltage. Later, this method of Boor and Muller was used by others<sup>11–13</sup> to measure  $S$  from 300 to 620 K. Furthermore, Kumar *et al.*<sup>14</sup> utilized this method for measuring  $S$  in the temperature range 80–650 K. In the earlier works,<sup>11–13</sup> the attachment of the thermocouple with the copper block has been made with silver paste. Above 620 K, this contact breaks down and measurement can no longer be done. Therefore, inserting the thermocouple to copper blocks is one of the challenges to fabricate the instrument for measuring  $S$  at high temperatures. Apart from this, the making of a heater is another challenge for high temperature applications. Keeping these challenges in mind, here, we have fabricated the instrument using the method proposed by Boor and Muller<sup>10</sup> to measure  $S$  in the temperature range 300–800 K. We have fixed the thermocouple with the help of a fire gun and using a thin wire of a specially designed material containing 95% silver and 5% zinc. Details of welding of the thermocouple and making of the heater are described in Sec. III.

In a more general way,  $\kappa$  is defined as the ability of materials to conduct heat. Various methods have been developed for the measurement of  $\kappa$ . These methods have their own merits and demerits.<sup>15</sup> The accurate measurement of  $\kappa$  is always a difficult process due to complexities involved in the quantification of heat flow through sample. The existing  $\kappa$  measurement techniques are broadly classified into two categories: steady-state and non-steady-state. In steady-state, measurement is carried out when the temperature of the material at a particular position does not vary with time. The non-steady-state method takes less time for the measurement because this method does not have the requirement to wait for the steady-state. The laser flash method developed by Parker *et al.*<sup>16</sup> is most popular among the non-steady-state-based techniques. However, this method has been tested only for metals around room temperature. Another popular technique is the  $3\omega$  method, which has been mainly developed to measure the thermal conductivity of thin films and thin wires.<sup>15,17,18</sup> In this method, a frequency of  $\omega$  is used to excite the heater and then  $\kappa$  is measured from the  $3\omega$  response.

The signal analysis in the non-steady-state method is quite heavy, while the steady-state method involves easy signal analysis. The available steady-state-based methods are axial heat flow, guarded hot plate, direct electrical heating, hot wire method, etc.<sup>15</sup> In steady-state methods, one-dimensional Fourier's law of heat

conduction is employed to measure  $\kappa$ . The measurement accuracy of this method totally depends on how accurately one measures the amount of heat passing through the sample. This is because heat is lost through conduction, convection, and radiation, which becomes more significant at high temperatures.<sup>9</sup> The undefined amount of heat loss is measured in different ways. For example, Zawilski *et al.*<sup>19</sup> described a parallel thermal conductance technique for measuring  $\kappa$ , where heat loss is determined by running the instrument without a sample. They measured  $\kappa$  from room temperature to 12 K. Later, Dasgupta and Umarji<sup>7</sup> implemented this technique to measure  $\kappa$  from room temperature to 700 K. A wide variation of  $\kappa$  is reported at room temperature only. They reported the  $\kappa$  value of CrSi<sub>2</sub> from room temperature to 650 K with the maximum value of ~2.2 W/m K. Recently, Patel and Pandey<sup>20</sup> fabricated the instrument for measuring  $\kappa$  using the same technique of parallel thermal conductance. However, their instrument is limited to measuring  $\kappa$  from room temperature to 620 K. Needless to say, heat loss increases with an increase in the temperature, and measurement of  $\kappa$  at high temperatures becomes more challenging. Keeping this in mind, we have fabricated the instrument by making a very thin heater and insulating heater base to minimize the heat loss. The instrument is tested in the temperature range of 300 to 800 K for measuring a wide range of  $\kappa$  values with standard samples. The speciality of this instrument is that it can measure  $S$  as well as  $\kappa$  simultaneously.

Data collection productivity is greatly improved by using automated systems that can obtain  $S$  and  $\kappa$  values at multiple temperature levels and ranges. Manual data collection is a troublesome process when the measurement is carried out for a long span of time. In this regard, we can say that manual monitoring of  $S$  and  $\kappa$  is a restless and time taking process when these measurements are performed in a steady-state and wide temperature range. In the present study, our instrument facilitates the simultaneous measurement of  $S$  and  $\kappa$  in the steady-state and in a wide temperature range. Here, simultaneous measurement saves time, but it requires a number of output signals to be collected by maintaining the thermal stability, which increases the difficulty for a user. Therefore, to make the process easier, automation of measurement can be done where these complexities are taken into account. One of the popular interfacing tools is LabVIEW. However, LabVIEW is a commercially paid graphical language. So, to avoid the retail cost, we have automated the measurement with the open-source "Python" programming language. Python has vast libraries support, which evades the dependency on external libraries.

In this work, we have designed and fabricated a simple and low-cost instrument for the simultaneous measurement of  $S$  and  $\kappa$  in the temperature range 300–800 K. The differential method has been implemented for measuring  $S$ , whereas the parallel thermal conductance technique is used for the measurement of  $\kappa$ . All parts of the sample holder are easily available in the market and can be replaced as per the user's interest. This instrument can be used for samples with various dimensions and shapes. The instrument is tested by performing the measurement on the standard samples of nickel, gadolinium, Fe<sub>2</sub>VAL, and LaCoO<sub>3</sub>. A wide range of  $S$  values from ~−20 to ~600  $\mu\text{V/K}$  and  $\kappa$  values from ~1.1 to ~23.5 W/m K are measured using our instrument. The measured values are in good agreement with the reported data. The instrument is automated with open-source programming language Python to minimize human effort.

## II. FORMULATIONS OF MEASUREMENT

In this section, we discuss the formulations used for the measurement of  $S$  and  $\kappa$  in the present study.

### A. Measurement of Seebeck coefficient

Here, the differential method proposed by de Boor and Muller<sup>10</sup> has been implemented to measure  $S$ . In this method,  $S$  of a sample is calculated by

$$S = -\frac{U_{neg}}{U_{pos} - U_{neg}} S_{TC}(\bar{T}) + S_{neg}(\bar{T}), \quad (2)$$

where  $U_{pos}$  and  $U_{neg}$  are the voltages measured across the positive legs and negative legs of thermocouple wires, respectively.  $S_{TC} = S_{pos} - S_{neg}$  is the Seebeck coefficient of the thermocouple, where  $S_{pos}$  and  $S_{neg}$  are the Seebeck coefficients of positive and negative legs of the thermocouple wires, respectively.  $\bar{T} = (T_1 + T_2)/2$  is the absolute temperature, where  $T_1$  and  $T_2$  are the temperatures of the hot and cold sides, respectively. Two K-type thermocouples are used to measure  $T_1$ ,  $T_2$ ,  $U_{pos}$ , and  $U_{neg}$ , as shown in Fig. 1. Here, it is important to note that the temperature dependency of  $S_{TC}$  and  $S_{neg}$  has been taken care of in the present study.

### B. Measurement of thermal conductivity

Steady-state-based Fourier's law of thermal conduction is used for the measurement of  $\kappa$ . In this method,  $\kappa$  of a material is calculated as

$$\kappa = \frac{\dot{Q}_s}{A \cdot \Delta T}, \quad (3)$$

where  $\dot{Q}_s$  is the amount of heat passing through the cross-sectional area  $A$  of the sample per unit time.  $\Delta T$  is the temperature gradient across the thickness  $l$  of the sample. The accuracy of the measurement of  $\kappa$  totally depends on how accurately we measure  $\dot{Q}_s$ . However, the quantification of  $\dot{Q}_s$  is not straightforward due to the

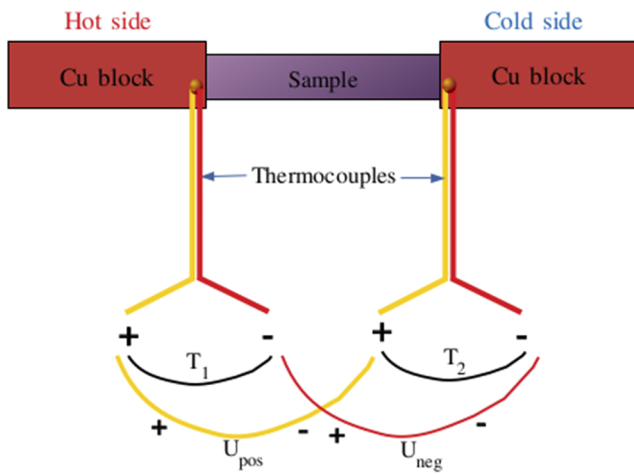


**FIG. 1.** Wiring scheme for the measurement of  $T_1$ ,  $T_2$ ,  $U_{pos}$ , and  $U_{neg}$  using thermocouples.

undefined amount of heat loss during the heat transfer process. In the present work, the amount of heat loss is measured by the parallel thermal conductance technique given by Zawilski *et al.*<sup>19</sup> as discussed in Sec. I. To minimize the heat loss, we have made a thin heater, which is fixed on insulating blocks as shown in Fig. 2. At the first step, heat loss is recorded by running the instrument without a sample. In this case, heat loss occurs through conduction loss through insulator blocks and radiation loss from the surfaces of the copper block as shown in Fig. 2(a). For a given input power, the temperature initially increases linearly as a function of time as the heat loss is less. Afterward, heat loss increases as the temperature increases. Eventually, both the input power and heat loss rate become equal at equilibrium. At this condition, the temperature is recorded and the corresponding input power is noted as baseline correction. Then, at the next step, the sample is placed on a copper block and power is delivered to the heater. In this case, heat generated by the heater is distributed through insulating blocks as well as through the sample as shown in Fig. 2(b). If the same temperature is maintained in both the steps, then the input power difference between these two steps (with sample–without sample) will give the net power flowing through the sample. Therefore, net heat flow through the sample is mathematically defined as

$$\dot{Q}_s \approx P_{in} - P_l, \quad (4)$$

where  $P_{in}$  is the power delivered to the heater when the sample is placed and  $P_l$  is the baseline power supplied to the heater with an empty sample.  $\dot{Q}_s$  is used in Eq. (3) to calculate  $\kappa$ . At this point, it is important to note that heat loss through side walls of the sample is ignored, since this loss is generally expected to be negligibly small as compared to heat flow through the sample.<sup>9</sup>

## III. APPARATUS DESCRIPTION

A schematic diagram of the instrument is shown in Fig. 3(a). Different components are labeled by numbers. For the better visualization of the measurement setup, a real image of the sample holder is inserted, as shown in Fig. 3(b). In the figure, sample (5) is placed between the copper blocks (17) and (18) of cross-sectional area  $8 \times 8 \text{ mm}^2$  and thickness 3 mm. Two K-type thermocouples (7) and (8) of 30 swg are welded at the side wall of the copper blocks. Welding is done with the help of a fire gun and using a thin wire of a specially designed material for this purpose having a mixture of 95% silver and 5% zinc. At the time of welding, if heat is provided to the copper block and thermocouple junction for a long time, it will make the thermocouple little brittle and may break after a few measurements. So, to make it robust, we need to cover the thermocouple with glass wool or ceramic tube at the time of welding. In addition to this, welding should be done very carefully to minimize the thermal contact resistance at the interfaces, which may affect the actual  $\Delta T$  of the sample. To minimize the unnecessary creation of  $\Delta T$  across the copper blocks, both the thermocouples are embedded as close as possible to the sample (about 0.2 mm apart from the surface). We know that copper is a good conductor of heat (thermal conductivity  $\sim 400 \text{ W/m K}$  at room temperature). Therefore, it is expected that the temperature gradient due to copper blocks is negligible as compared to the temperature gradient of thermoelectric materials. Here, it should be mentioned that galinstan (GaInSn) liquid metal eutectic alloy has been used between the copper block and sample

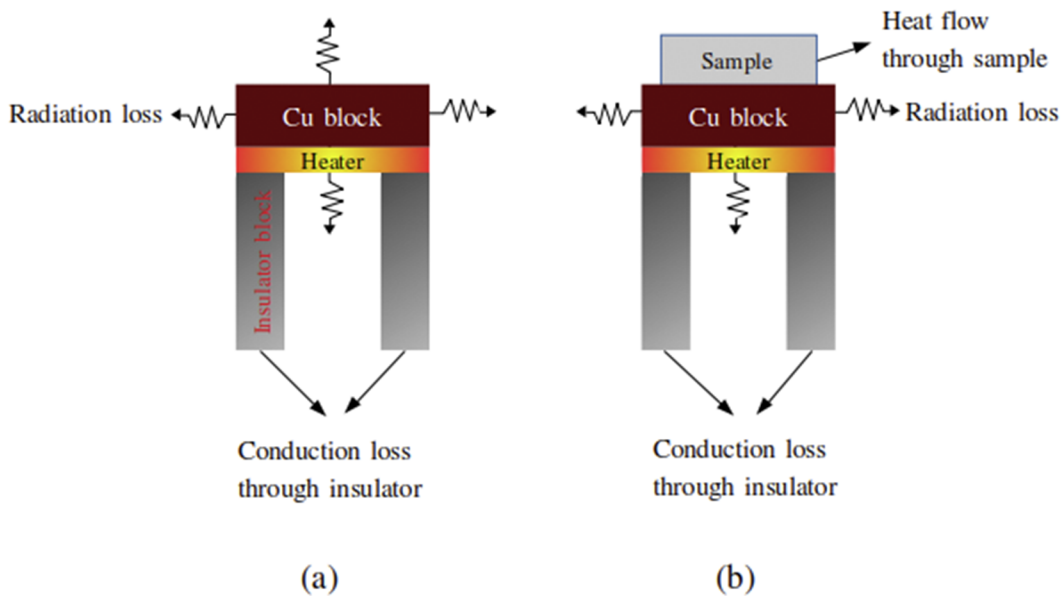


FIG. 2. Schematic diagram of heat flow: (a) without sample and (b) with sample.

to ensure proper thermal contact. The boiling point of galinstan is  $\sim 1800$  K, which makes it suitable for high-temperature applications. However, galinstan should not be used for the case where material is highly reactive with galinstan.

A thin heater (6) of  $24\ \Omega$  is used to heat the sample. This heater is made by winding the Kanthal wire of 40 swg over a mica sheet of dimensions  $10 \times 8 \times 0.2\ \text{mm}^3$  (length  $\times$  width  $\times$  thickness). This heater is coated with high-temperature cement and wrapped by

another mica sheet to avoid electrical contact. Then, it is covered by a copper sheet of thickness 0.4 mm and welded to the copper block (17) over which the sample is placed. The copper wire (16) is used to supply the current to the heater. The heater is placed over two insulating gypsum blocks (9) using high-temperature cement. The thermal conductivity of the gypsum block is very low  $\sim 0.017\ \text{W/m K}$  at 300 K and also suitable for high-temperature applications.<sup>21</sup> The dimensions of each gypsum block are  $8 \times 2 \times 25\ \text{mm}^3$ . A finite gap

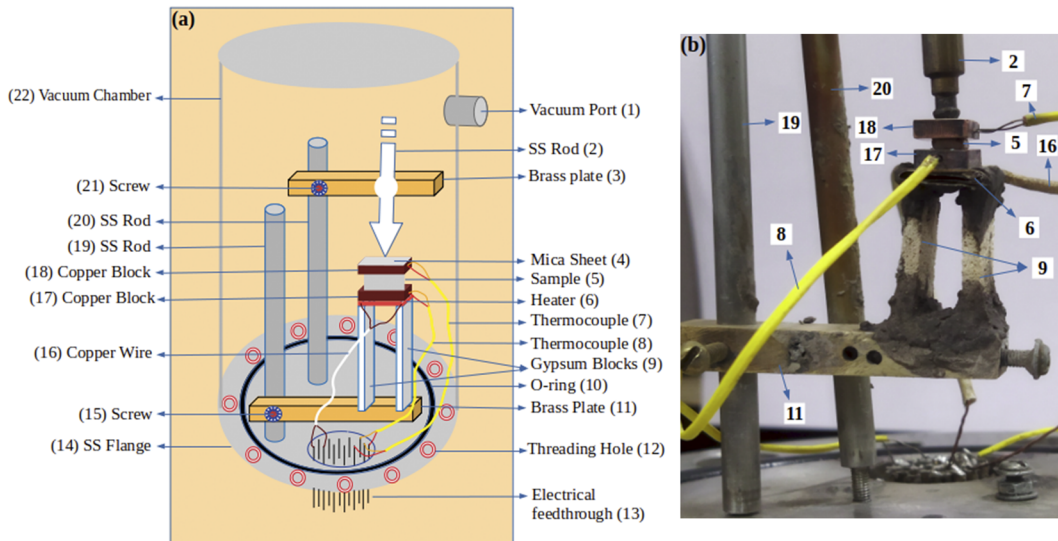


FIG. 3. (a) Schematic diagram of the measurement setup. (b) Real image of the sample holder.

between two gypsum blocks has been kept to minimize the conduction loss through the gypsum block. These gypsum blocks have been made to stand on a brass plate (11). This brass plate is supported with a stainless steel (SS) rod (19) using a screw (15). A mica sheet (4) is laid on the cold side copper plate (18) to insulate the sample electrically. An SS rod (2) having threads is used to apply the pressure on the sample, which is screwed with a brass plate (3). This brass plate (3) is supported by an SS rod (20) using a screw (21). Both the SS rods (19) and (20) are attached to the SS flange (14). A circular O-ring (10) is used for proper vacuum seal of the chamber.

The whole assembly of the sample holder is mounted on the SS flange (14) and then covered by an SS made cylindrical vacuum chamber (22) using nut bolts through holes (12). The inner diameter and length of the vacuum chamber are  $\sim 10$  and  $\sim 30$  cm, respectively. A port (1) of size KF-25 is used to connect the sample's chamber to the vacuum pump. The electrical feedthrough (13) is used for electrical communication between inside and outside the vacuum chamber.

#### IV. SAMPLE DIMENSION

The measurement of  $S$  can be carried out for any sample irrespective of its dimensions. However, for  $\kappa$ , proper sample dimensions are required as the thickness and cross-sectional area are used for  $\kappa$  measurement. The cylindrical and rectangular shaped samples are used in the present study. Top and bottom surfaces of the sample should be parallel to make good contact of the sample with the copper block. The pellet of the sample should be as compact as possible for the measurement.

#### V. MEASUREMENT PROCEDURE

At first, the measurement of heat loss has to be done before loading the sample. Here, it is important to note that at the time of heat loss measurement, top copper block (18) is placed at the ground of the measurement setup. Once heat loss measurement is performed, the sample (5) is mounted between the copper blocks (17) and (18). We should ensure that both the surfaces of the sample are in proper contact with the copper blocks. A small amount of galinstan is used at the interface of the sample and copper block to

secure the proper heat transfer. Then, the vacuum chamber (22) is evacuated using a vacuum pump. A Keithley sourcemeter 2604B is used to feed the current to the heater. Once the heater is set on, the copper blocks (17) start getting heated and heat passing through the sample depends on the thermal conductivity of the sample. As soon as the steady-state is reached, the thermocouples (8) and (7) measure the hot side and cold side temperatures, respectively. Then, the average temperature of the hot and cold sides gives  $T_{avg}$  of the sample. Subsequently, power supplied to the heater is increased for the next  $T_{avg}$  of the sample and so on. This is how sample's temperature is raised to 800 K. Various output signals ( $T_1$ ,  $T_2$ ,  $U_{pos}$ ,  $U_{neg}$ , etc.) are measured by using a Keithley digital multimeter 2002 with a multichannel scanner card. The sourcemeter and multimeter are interfaced with a computer using an IEEE-488B interface bus. It is essential to mention that the measurement of  $S$  and  $\kappa$  for a given sample is carried out simultaneously.

The whole measurement process is automated with the open-source programming language "Python." The program is given as the [supplementary material](#). The PyVISA, NumPy, and matplotlib libraries are utilized in the program. The user only needs to define the input parameters, and no further interaction of the user is required until the measurement gets completed. As per the input power defined, the sourcemeter provides current to the heater and waits for steady-state. Steady-state is defined by monitoring the rate of change of  $T_h$ . This rate of change of  $T_h$  is set as 0.006 K, which is checked in every 5 s. Once the steady-state criteria are fulfilled five times successively, the multimeter measures the output signals. When the heating cycle reaches its defined maximum temperature limit, the heating loop breaks and the next loop for cooling starts to cool the sample. During the cooling period, the power in each cycle decreases with a defined step size until the sample again returns to room temperature. Data are also collected in the cooling cycle similar to the heating process. Equations (2) and (3) are used in the Python program to calculate  $S$  and  $\kappa$ , respectively. Here, it is important to note that the temperature dependence of  $S_{TC}$  and  $S_{neg}$  has been implemented in the program using the interpolation method. The raw values of  $S_{TC}$  and  $S_{neg}$  are taken from the literature.<sup>10,22</sup> During the measurement, the user can observe all the necessary parameters graphically, as the real-time plotting has been employed using the matplotlib library. All the measured quantities along with input parameters are saved to (file name).csv file. The live data

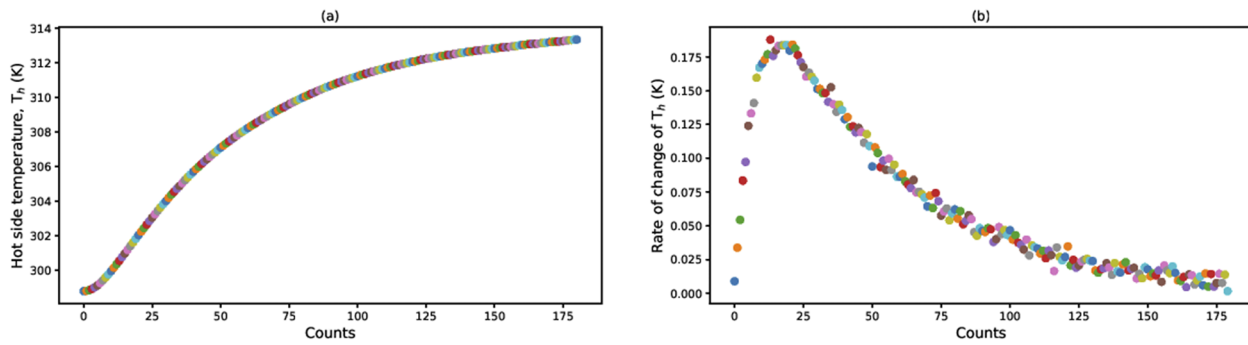


FIG. 4. Screenshot of live data: (a) change in the hot side temperature ( $T_h$ ) with counts and (b) rate of change of  $T_h$  with counts. One count takes 5 s.

for acquiring steady-state are shown in Fig. 4. Figure 4(a) represents the increase in the hot side temperature with counts, while Fig. 4(b) exhibits the rate of change of the hot side temperature with counts. Each count takes 5 s. Hence, for a single data point, it takes around 15 min.

## VI. RESULTS AND DISCUSSION

### A. Heat loss measurement

Before carrying the measurement of the sample, the heat loss measurement is taken for  $\kappa$ . Figure 5 shows the heat loss as a function of hot side temperature ( $T_h$ ). The reliability of the  $\kappa$  value significantly depends on how accurately the heat loss value is measured. Keeping this in mind, we have made a thin heater to minimize the heat loss and to achieve the required temperature easily. Figure 5 shows that heat loss is quite low at the beginning. As the temperature increases, heat loss also increases non-linearly. This non-linear increment is fitted with a polynomial of quartic degree: heat loss =  $aT + bT^4$ . Here, values of  $a$  and  $b$  are taken as 0.959 mW/K and  $1.566 \times 10^{-8}$  mW/K<sup>4</sup>, respectively. The first term indicates convection loss where heat loss depends on temperature linearly. The quartic term signifies the radiation loss in a high-temperature region, which is confirmed by Stefan's law:  $E = \sigma T^4$  ( $E$  is the radiant heat energy and  $\sigma$  is Stefan's constant). The purpose of this polynomial fit is that (i) users can get heat loss at any value of temperature in between 300–800 K and (ii) the heat loss value above 800 K can also be calculated.

### B. Seebeck coefficient measurement

The instrument is validated by measuring  $S$  of different samples with different dimensions in the temperature region 300–800 K. In order to check the flexibility of the instrument, measurements of various classes of samples having a wide range of  $S$  are carried out. Figure 6 shows the measured values of  $S$  for nickel, Fe<sub>2</sub>VAI, and LaCoO<sub>3</sub> (LCO1) as a function of temperature. The shapes and dimensions of these samples are tabulated in Table I.

Figure 6(a) shows the measured values of  $S$  as a function of temperature of high purity (99.99%) nickel. The value of  $S$  at 300 K is

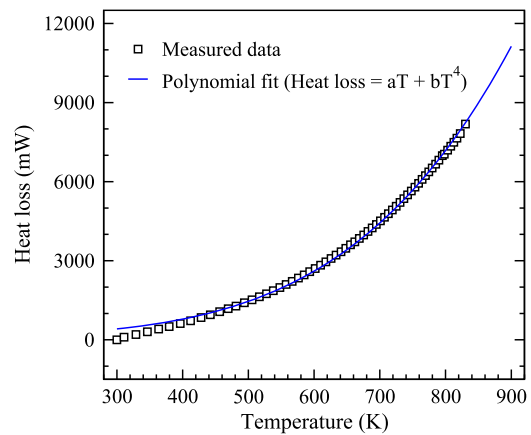


FIG. 5. Heat loss as a function of temperature at the hot side.

found to be  $\sim -19.2 \mu\text{V/K}$  and then decreases up to  $\sim 490 \text{ K}$  with the corresponding value of  $\sim -24.4 \mu\text{V/K}$ . After 490 K,  $S$  increases monotonically until  $\sim 660 \text{ K}$  and attains the value of  $\sim -18.9 \mu\text{V/K}$ . The value of  $S$  continuously decreases above 660 K and reaches  $\sim -22.9 \mu\text{V/K}$  at 800 K. In order to verify, we have compared our  $S$  with the reported data of Burkov *et al.*<sup>23</sup> and Ponnambalam *et al.*<sup>24</sup> in the same figure. The  $S$  value matches well with the reported data, and the maximum deviation in the results is found to be  $\sim 1 \mu\text{V/K}$  in the considered temperature range.

Figure 6(b) exhibits the temperature dependence of  $S$  for Fe<sub>2</sub>VAI. This compound possesses a deep pseudogap at the Fermi level, and due to this, it is known to give large values of  $S$  and  $\sigma$ .<sup>25,26</sup> This compound has been synthesized by the arc melting technique.<sup>27</sup> The value of  $S$  is observed to be  $\sim -138 \mu\text{V/K}$  at 300 K. Furthermore, the magnitude of  $S$  is found to be monotonically decreasing until the highest temperature of interest. At 800 K,  $S$  is found to be  $\sim -18 \mu\text{V/K}$ . Our result is compared with the reported data by Sk *et al.*<sup>27</sup> and Kurosaki *et al.*<sup>28</sup> as shown in the same figure. From the figure, one can notice that our data are in good agreement with

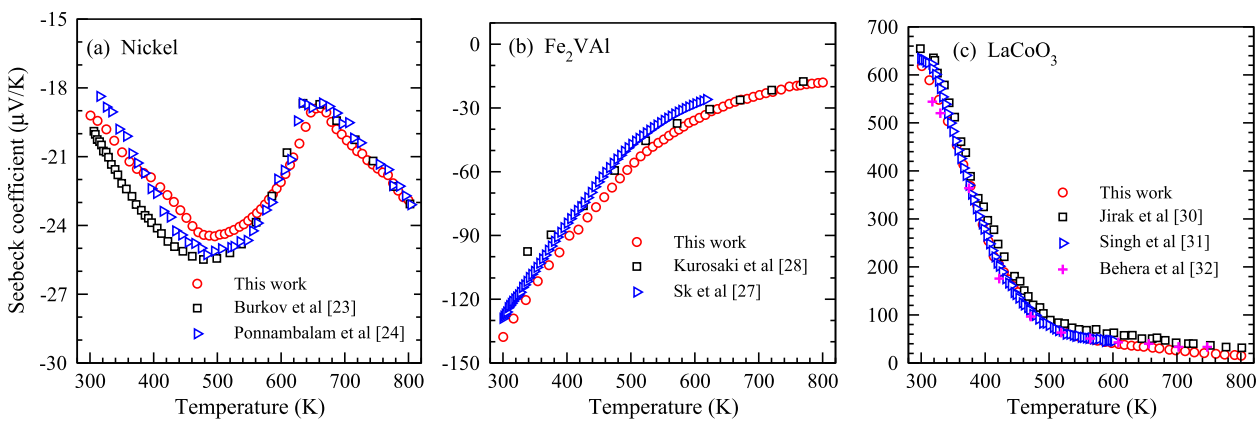


FIG. 6. Seebeck coefficient of (a) nickel, (b) Fe<sub>2</sub>VAI, and (c) LaCoO<sub>3</sub> as a function of temperature.

**TABLE I.** Shapes and dimensions of the test samples.

Sample name	Shapes of cross section	Thickness (mm)	Cross-sectional area (mm <sup>2</sup> )
Nickel	Circular	2.0	28.27
Gadolinium	Rectangular	0.7	4.86
Fe <sub>2</sub> VAL	Rectangular	1.38	15.0
LaCoO <sub>3</sub> (LCO1)	Rectangular	0.5	24.0
LaCoO <sub>3</sub> (LCO2)	Circular	1.0	50.27

the reported data throughout the temperature range. However, at low temperatures, the obtained values of  $S$  slightly deviate from the results mentioned in the work of Kurosaki *et al.*<sup>28</sup> However, this deviation vanishes as the temperature increases. The possible reason for this deviation may be the use of different annealing temperatures for the synthesis of compounds in the respective works.

The  $S$  value of LaCoO<sub>3</sub> is measured in the temperature region 300–800 K, which is displayed in Fig. 6(c). This compound is synthesized by the combustion technique. LaCoO<sub>3</sub> gives a large  $S$  at 300 K,<sup>29,30</sup> which is a good signature for an efficient TE material. At 300 K,  $S$  is found to be  $\sim 618 \mu\text{V/K}$  and then decreases continuously throughout the full temperature range as shown in Fig. 7(c). At 800 K, the observed value of  $S$  is  $\sim 15 \mu\text{V/K}$ . The figure shows that the magnitude of  $S$  decreases rapidly as the temperature increases from 300 to  $\sim 500$  K. After 500 K, this decrement rate falls down and continues up to 800 K. In the temperature interval  $\sim 300$  to 500 K, the change in  $S$  is  $\sim 535 \mu\text{V/K}$  with a decrement rate of  $2.67 \mu\text{V/K}$ . From 500 to 800 K, this change in  $S$  is observed to be  $\sim 68 \mu\text{V/K}$  with a decrement rate of  $0.23 \mu\text{V/K}$ . A similar trend of  $S$  is reported by other groups,<sup>30–32</sup> which are also shown in the figure. In the full studied temperature range, our  $S$  value is in good agreement with the reported data.

Among the test samples used here, nickel is a pure metal, Fe<sub>2</sub>VAL is an inter-metallic Heusler compound, and LaCoO<sub>3</sub> is an oxide perovskite material. Hence, measurements of  $S$  on various kinds of materials are carried out in the present study. This suggests

that our setup can be used to measure  $S$  in the temperature range 300–800 K for any class of materials having a wide range of  $S$  values.

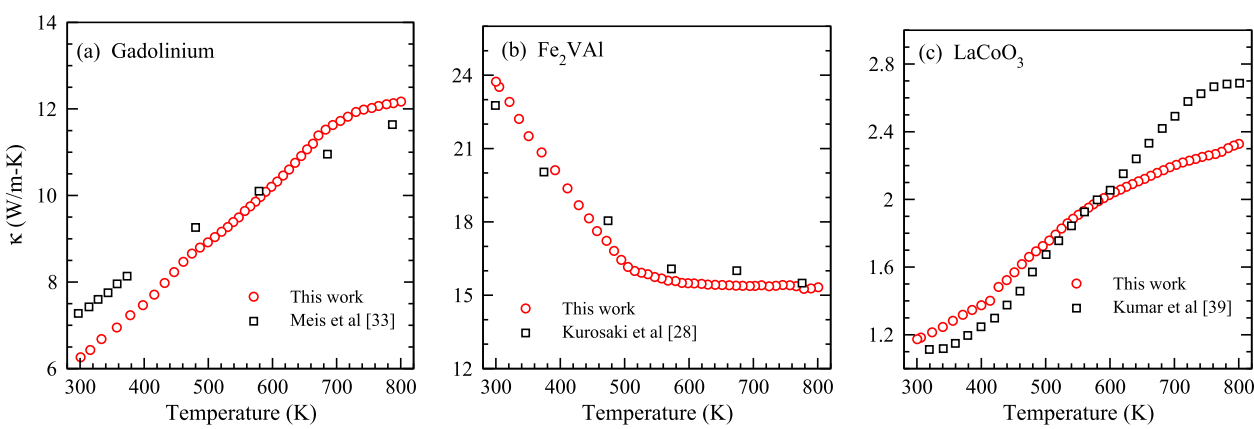
### C. Thermal conductivity measurement

To examine our setup, we have measured  $\kappa$  of gadolinium, Fe<sub>2</sub>VAL, and LaCoO<sub>3</sub> (LCO1) in the temperature range 300–800 K as shown in Fig. 7. The shapes and dimensions of these samples are shown in Table I. The thickness and cross-sectional area of the sample are important for the measurement of  $\kappa$ .

Figure 7(a) represents the measured  $\kappa$  for gadolinium as a function of temperature. Gadolinium has one of the lowest  $\kappa$  values among the metallic compounds.<sup>33</sup> From Fig. 7(a),  $\kappa$  is observed to increase with increasing temperature. The values of  $\kappa$  are found to be  $\sim 6.3$  and  $\sim 12.2 \text{ W/m K}$  at 300 and 800 K, respectively. The obtained values of  $\kappa$  are compared with the reported data of Meis *et al.*<sup>33</sup> as shown in the same figure. The  $\kappa$  value of gadolinium at room temperature is highly controversial. This is because, around room temperature, gadolinium possesses the critical ferromagnetic ( $16^\circ\text{C}$ ) and paramagnetic ( $25$ – $29^\circ\text{C}$ ) phases.<sup>34</sup> In  $18$ – $25^\circ\text{C}$ , the values of  $\kappa$  measured using different methods are reported from  $6.6$  to  $14 \text{ W/m K}$  in different literature studies.<sup>33,35–37</sup> Figure 7(a) shows that in a lower temperature region, both the data are little deviating, while this deviation diminishes in a high-temperature region.

Figure 7(b) illustrates the temperature dependence values of  $\kappa$  for Fe<sub>2</sub>VAL. The value of  $\kappa$  at 300 K is found to be  $\sim 23.5 \text{ W/m K}$ . From temperature 300 to  $\sim 500$  K,  $\kappa$  decreases drastically and then it is almost constant throughout the remaining temperature range. At 800 K, the observed value of  $\kappa$  is  $\sim 15.3 \text{ W/m K}$ . In the temperature range 300–500 K, the change in the magnitude of  $\kappa$  is  $7 \text{ W/m K}$ , whereas this value is  $1 \text{ W/m K}$  in the temperature range 500–800 K. Our  $\kappa$  matches well with the reported value of Kurosaki *et al.*<sup>28</sup> in the whole temperature region as shown in the figure.

We have also carried out the measurement of  $\kappa$  for the oxide sample. Oxide samples are known for having low values of  $\kappa$ . The temperature dependence of  $\kappa$  for LaCoO<sub>3</sub> is shown in Fig. 7(c). The value of  $\kappa$  is measured to be  $\sim 1.2 \text{ W/m K}$  at 300 K, and then, it increases monotonically up to 800 K with the corresponding value of  $\kappa$  of  $\sim 2.3 \text{ W/m K}$ . The figure shows that the  $\kappa$  value increases

**FIG. 7.** Temperature dependence of the thermal conductivity of (a) gadolinium, (b) Fe<sub>2</sub>VAL, and (c) LaCoO<sub>3</sub>.

almost linearly up to  $\sim 500$  K and then becomes saturated as the temperature increases. The values of  $\kappa$  around room temperature are reported from 0.38 to 3.2 W/m K in different works.<sup>32,38–42</sup> We know that  $\kappa$  depends on the particle size as well as porosity of the sample. Therefore, this difference is maybe because the sample has been synthesized by different techniques and  $\kappa$  is measured by various methods in the respective works.<sup>32,38–42</sup> Our  $\kappa$  comes out to be in good agreement with the reported value of Kumar *et al.*<sup>39</sup> as shown in the figure. A small deviation is observed at high temperatures. The maximum deviation of 0.36 W/m K is found at 800 K.

In order to check the thickness and geometry effect of the sample on  $S$  and  $\kappa$ , we have performed the measurements as shown in Fig. 8. For this, we have chosen two LaCo<sub>3</sub> samples with different thicknesses and geometries, which are named as LCO1 and LCO2. The dimensions of these samples are provided in Table I. Figure 8(a) shows the measurement of  $S$ . The  $S$  value of LCO1 is slightly higher than that of LCO2. The deviations of  $|S|$  between LCO1 and LCO2 are found to be  $\sim 17.6$  and  $\sim 0.78$   $\mu\text{V/K}$ , which correspond to 2.9% and 5.3% at 300 and 800 K, respectively. Here, it is important to note that the creation of  $\Delta T$  in the present instrument depends on the thermal conductivity and thickness of the samples, as we are not controlling  $\Delta T$ . Therefore,  $\Delta T$  of LCO2 (higher thickness)

will be high as compared to that of LCO1 (lower thickness). The final  $S$  of the sample is measured by averaging the sample's hot and cold end temperatures. Hence, a different  $\Delta T$  for a given sample (with constant input power) with a different thickness affects the value of  $S$ . Figure 8(b) displays the measurement of  $\kappa$  of LCO1 and LCO2. The  $\kappa$  value of LCO2 is slightly higher than that of LCO1. The deviations of  $|\kappa|$  between LCO1 and LCO2 are found to be  $\sim 0.04$  and  $\sim 0.0.09$  W/m K, which correspond to 3.4% and 3.8% at 300 and 800 K, respectively. From the figure, it is clear that the deviation of  $|\kappa|$  increases slightly as the temperature increases. One of the reasons for this deviation can be attributed to the more radiation loss of the side walls of the thicker sample. Therefore, for the precise measurement of  $\kappa$  for a thick sample, one should also consider the radiation loss from the side walls of the sample. Capturing this radiation loss is really a difficult process as it depends on the sample's thickness. Therefore, using a lower thickness sample is advisable to obtain a more accurate value of  $S$  and  $\kappa$  in this instrument.

Various types of samples are tested for  $\kappa$  measurement using our instrument with a wide range of  $\kappa$  values from  $\sim 1.1$  to  $\sim 23.5$  W/m K. The instrument is also examined for a wide range of  $S$  values from  $\sim -20$  to  $\sim 600$   $\mu\text{V/K}$ . Therefore, this study proposes that the present apparatus can be used for the simultaneous measurement of  $S$  and  $\kappa$  in the temperature range 300–800 K. At this point, it is important to mention that in metallic samples, the creation of  $\Delta T$  is low and hence the voltage difference due to this  $\Delta T$  will also be low. Therefore, a small error in the measurement of  $\Delta T$  and voltage across the sample will significantly affect the value of  $S$  and  $\kappa$ . Therefore, this instrument may not be suitable for materials possessing extremely low  $S$  or very high  $\kappa$ . Finally, we have calculated the precision of the measurements of  $S$  and  $\kappa$  by taking multiple readings on the same sample with fixed contact. The precision is found to be in the range of  $\sim 1\%$  to  $2\%$  in the entire temperature range. We know that the accuracy of the measurement of  $S$  and  $\kappa$  is generally affected by the inherent defects present in the sample, different synthesis conditions, porosity of the sample, etc. Therefore, by observing the comparison of our data with the reported values, one can conclude that this instrument is reliable for the simultaneous measurement of  $S$  and  $\kappa$  in the temperature range 300–800 K.

The salient features of our instrument are making the sample platform by introducing a thin heater, attachment of TCs to the copper block, interfacing the measurement with Python programming, etc. The components used to fabricate the sample holder are easily available in the market (also cheap) and simple to replace. Apart from this, the interfacing of the measurement with Python is one of the key factors and may be helpful for those who are interested to work in this area. The salient features of this program are: free to access, the program uses a lower number of libraries, user-interactive, and it requires a lower number of input parameters and hence it is easy to implement.

## VII. CONCLUSIONS

In conclusion, we have fabricated the instrument for measuring the Seebeck coefficient ( $S$ ) and thermal conductivity ( $\kappa$ ) simultaneously in the temperature range 300–800 K. A simple, low-cost, and user-friendly instrument is fully automated with open-source

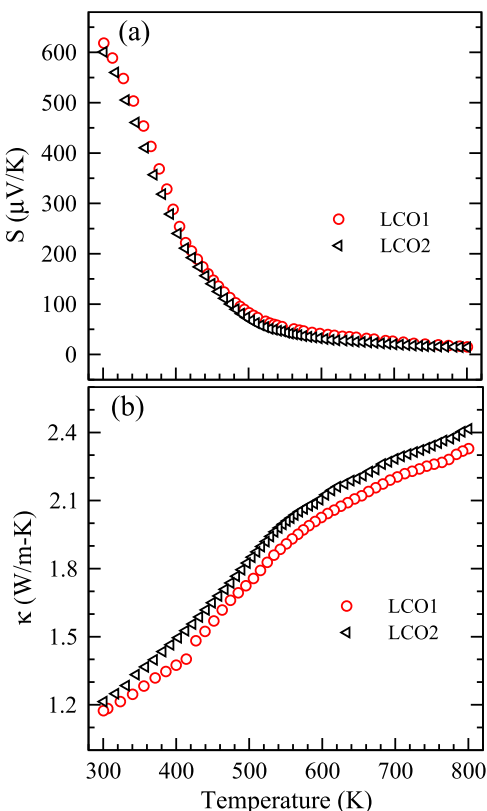


**FIG. 8.** Temperature dependent (a) Seebeck coefficient and (b) thermal conductivity of LaCo<sub>3</sub> with different thicknesses and geometries. Dimensions of LCO1 and LCO2 are provided in Table I.

programming language Python. The differential method is used for  $S$  measurement, where the same thermocouple is employed to measure temperature as well as voltage. Temperature dependent  $S$  of the thermocouple has been taken care of. The parallel thermal conductance technique is used for heat loss measurement. Steady-state-based Fourier's law of thermal conduction is used for the measurement of  $\kappa$ . We have made a thin heater and insulating heater base to minimize the heat loss. Making the sample platform, thin heater, and attachment of thermocouples to the copper block are major components to make this instrument robust and high-temperature measurement. All the components for making the sample holder, e.g., copper block, thermocouple, gypsum block, brass plate, SS rod, and mica sheet, are easily available in the market and can be replaced as per the requirements. The instrument is validated by performing measurements on various kinds of samples having different dimensions and shapes. The measurements on test samples, such as nickel, gadolinium,  $\text{Fe}_2\text{VAl}$ , and  $\text{LaCoO}_3$ , are carried out. The instrument is tested for a wide range of  $S$  values from  $\sim -20$  to  $\sim 600 \mu\text{V/K}$  and  $\kappa$  values from  $\sim 1.1$  to  $\sim 23.5 \text{ W/m K}$ . The measured values are found to be in good agreement with the reported values. The simplicity and cost-effective impact of our instrument will be useful for people in the field of thermoelectric for high-temperature  $S$  and  $\kappa$  measurements.

## SUPPLEMENTARY MATERIAL

See the [supplementary material](#) of the interfacing code (written in Python language) for the simultaneous measurement of the Seebeck coefficient and thermal conductivity.

## AUTHOR DECLARATIONS

### Conflict of Interest

The authors have no conflicts to disclose.

## DATA AVAILABILITY

The data that support the findings of this study are available from the corresponding author upon reasonable request.

## REFERENCES

- <sup>1</sup>M. Akasaka, T. Iida, A. Matsumoto, K. Yamanaka, Y. Takanashi, T. Imai, and N. Hamada, *J. Appl. Phys.* **104**, 013703 (2008).
- <sup>2</sup>Y. Pei, H. Wang, and G. J. Snyder, *Adv. Mater.* **24**, 6125 (2012).
- <sup>3</sup>Y. Pei, X. Shi, A. LaLonde, H. Wang, L. Chen, and G. J. Snyder, *Nature* **473**, 66 (2011).
- <sup>4</sup>S. R. Sarath Kumar and S. A. Kasiviswanathan, *Rev. Sci. Instrum.* **79**, 024302 (2008).
- <sup>5</sup>C. Wood, A. Chmielewski, and D. Zoltan, *Rev. Sci. Instrum.* **59**, 951 (1988).
- <sup>6</sup>Z. Zhou and C. Uher, *Rev. Sci. Instrum.* **76**, 023901 (2005).
- <sup>7</sup>T. Dasgupta and A. M. Umarji, *Rev. Sci. Instrum.* **76**, 094901 (2005).
- <sup>8</sup>A. Muto, D. Kraemer, Q. Hao, Z. F. Ren, and G. Chen, *Rev. Sci. Instrum.* **80**, 093901 (2009).
- <sup>9</sup>R. Amatya, P. M. Mayer, and R. J. Ram, *Rev. Sci. Instrum.* **83**, 075117 (2012).
- <sup>10</sup>J. de Boor and E. Muller, *Rev. Sci. Instrum.* **84**(6), 065102 (2013).
- <sup>11</sup>A. Patel and S. K. Pandey, *Instrum. Sci. Technol.* **45**(4), 366 (2017).
- <sup>12</sup>S. Singh and S. K. Pandey, *Measurement* **102**, 26 (2017).
- <sup>13</sup>A. Patel and S. K. Pandey, *Instrum. Sci. Technol.* **46**(6), 600 (2018).
- <sup>14</sup>A. Kumar, A. Patel, S. Singh, A. Kandasami, and D. Kanjilal, *Rev. Sci. Instrum.* **90**(10), 104901 (2019).
- <sup>15</sup>X. C. Tong, "Characterization methodologies of thermal management materials," in *Advanced Materials for Thermal Management of Electronic Packaging* (Springer, New York, 2011), Vol. 30, pp. 59–129.
- <sup>16</sup>W. J. Parker, R. J. Jenkins, C. P. Butler, and G. L. Abbott, *J. Appl. Phys.* **32**, 1679 (1961).
- <sup>17</sup>A. J. G. Bourlon, "Thermal conductivity measurement by the  $3\omega$  method," Technical Note PR-TN 2005/01035, Philips Electronics, Koninklijke, 2005.
- <sup>18</sup>L. Lu, W. Yi, and D. L. Zhang, *Rev. Sci. Instrum.* **72**, 2996 (2001).
- <sup>19</sup>B. M. Zawilski, R. T. Littleton IV, and T. M. Tritt, *Rev. Sci. Instrum.* **72**, 1770 (2001).
- <sup>20</sup>A. Patel and S. K. Pandey, *Rev. Sci. Instrum.* **88**, 015107 (2017).
- <sup>21</sup>S. L. Manzello, S. Park, T. Mizukami, and D. P. Bentz, "Measurement of thermal properties of gypsum board at elevated temperatures," in Proceedings of the 5th International Conference on Structures in Fire (SiF'08) (Organising Committee, Fifth International Conference Structures in Fire (SiF'08) (Nanyang Technological University, Singapore, 2008), pp. 656–665.
- <sup>22</sup>R. E. Bentley, *Handbook of Temperature Measurement, The Theory and Practice of Thermolectric Thermometry* Vol. 3 (Springer, 1998).
- <sup>23</sup>A. T. Burkov, A. Heinrich, P. P. Konstantinov, T. Nakama, and K. Yagasaki, *Meas. Sci. Technol.* **12**, 264 (2001).
- <sup>24</sup>V. Ponnambalam, S. Lindsey, N. S. Hickman, and T. M. Tritt, *Rev. Sci. Instrum.* **77**, 073904 (2006).
- <sup>25</sup>Y. Nishino, S. Deguchi, and U. Mizutani, *Phys. Rev. B* **74**, 115115 (2006).
- <sup>26</sup>Y. Hanada, R. O. Suzuki, and K. Ono, *J. Alloys Compd.* **329**, 63 (2001).
- <sup>27</sup>S. Sk, P. Devi, S. Singh, and S. K. Pandey, *Mater. Res. Express* **6**, 026302 (2019).
- <sup>28</sup>K. Kurosaki, H. Muta, Y. Endo, A. Charoenphakdee, M. Uno, and S. Yamanaka, *J. Alloys Compd.* **486**, 507 (2009).
- <sup>29</sup>A. Maingan, D. Flahaut, and S. Hébert, *Eur. Phys. J. B* **39**, 145 (2004).
- <sup>30</sup>Z. Jirak, J. Hejtmek, K. Knek, and M. Veverka, *Phys. Rev. B* **78**, 014432 (2008).
- <sup>31</sup>S. Singh and S. K. Pandey, *Philos. Mag.* **97**(6), 451 (2017).
- <sup>32</sup>S. Behera, V. B. Kamble, S. Vitta, A. M. Umarji, and C. Shivakumara, *Bull. Mater. Sci.* **40**(7), 1291 (2017).
- <sup>33</sup>C. Meis, A. K. Froment, and D. Moulinier, *J. Phys. D: Appl. Phys.* **26**, 560 (1993).
- <sup>34</sup>P. Pascal, *Nouveau Traité de Chimie Minrale* (Masson et Cie, Paris, 1958), pp. 630–631.
- <sup>35</sup>S. Legvold and F. H. Spedding, ISC-508, 1954.
- <sup>36</sup>S. Arajs and R. V. Colvin, *J. Appl. Phys.* **35**, 1043 (1964).
- <sup>37</sup>R. W. Powell and B. W. Jolliffe, *Phys. Lett.* **14**, 171 (1965).
- <sup>38</sup>A. Cortes, J. S. T. Hernandez, J. F. Piamba, W. Lopera, and P. Prieto, *J. Supercond. Novel Magn.* **32**, 1367 (2019).
- <sup>39</sup>A. Kumar, K. Kumari, B. Jayachandran, D. Sivaprasadam, and A. D. Thakur, *J. Alloys Compd.* **749**, 1092 (2018).
- <sup>40</sup>F. Li, J.-F. Li, J.-H. Li, and F.-Z. Yao, *Phys. Chem. Chem. Phys.* **14**, 012213 (2012).
- <sup>41</sup>M. A. Bousnina, R. Dujardin, L. Perriere, F. Giovannelli, G. Guegan, and F. Delorme, *J. Adv. Ceram.* **7**(2), 160 (2018).
- <sup>42</sup>C. G. S. Pillai and A. M. George, *Int. J. Therm.* **4**, 183 (1983).